Journal of High School Science

Influence of solution chemistry on liquid-solid triboelectric charging of PTFE

Tang F

Submitted: December 20, 2025, Revised: version 1, January 28, 2026, version 2, January 28, 2026, version 3, February 13, 2026, version 4, February 28, 2026
Accepted: March 1, 2026

Abstract

Droplet-based TriboElectric NanoGenerators (TENGs) offer a simple and environmentally friendly way to convert liquid motion into electrical energy, yet the mechanisms that govern liquid–solid triboelectrification are still not fully understood. In particular, the role of solution chemistry in controlling charge generation remains unclear. In this work, we examine how pH, ionic strength, and molecular composition influence triboelectric charging when liquid droplets interact with a polytetrafluoroethylene (PTFE) surface in a controlled droplet-based TENG. Charge–time measurements were performed using acidic (acetic acid), basic (sodium acetate), mixed buffer, and ethanol–water solutions over a wide range of concentrations. Across all systems, increasing solute concentration reduced the magnitude of the accumulated charge. In electrolyte solutions, this suppression is consistent with enhanced interfacial screening, while in ethanol–water mixtures it arises from changes in dielectric properties and interfacial water structure. Acidic droplets exhibited a brief polarity reversal prior to reaching a negative steady-state plateau, suggesting that short-lived proton enrichment temporarily competes with electron transfer at early contact times. Overall, the results are most consistent with an electron transfer mechanism; however, electrokinetic contributions cannot be excluded. More experiments are needed to confirm the contribution mechanism.

Keywords

Triboelectricity, Triboelectric nanogenerators, Droplet-based energy harvesting, Solid-liquid triboelectrification, Triboelectric mechanisms, Nanotechnology, Interfacial electron transfer, Electric double layer, Debye screening, Liquid triboelectric series, Materials science, Acid-base interfacial chemistry

Faye Tang, William P. Clements High School, 4200 Elkins Rd, Sugar Land, TX 77479, USA.
faye.tang.r@gmail.com

https://doi.org/10.64336/001c.158503

1. Introduction

Harvesting energy from falling droplets is a simple yet powerful construct: converting what seems like a ubiquitous, unusable source of mechanical energy into usable electrical charge. Although individual droplets carry little momentum, their contact with solid surfaces can generate distinct bursts of triboelectric charge—turning rainstorms, condensation, and fluid motion into steady micro-scale power (1,2). This approach allows for an environmentally sustainable way for powering devices in places where conventional electricity is impractical. However, to turn droplet-based triboelectricity into a predictable and engineerable technology, its fundamental mechanisms must be far better understood than they are today.

TriboElectric (TE) charging is the process in which two uncharged objects gain electric charge through contact and subsequent separation—a phenomenon commonly observed when rubbing a balloon on hair or peeling a piece of tape from the dispenser (3). Despite its recognition since antiquity, with references as early as Plato's Timaeus in 300 B.C., the underlying mechanism of triboelectrification remains one of the least understood areas in electrostatics (3). Across physics, chemistry, and materials science, researchers have long attempted to identify which species—electrons, ions, radicals, or other intermediates—are transferred during the TE charging (3–9). Yet, progress has been hindered by the strong sensitivity of TE charging to environmental conditions, and scientists have surmised that even small variations can cause large errors in data and compromise overall reliability (9–11). Consequently, the precise identity of the transferred species that is responsible for this long-standing phenomenon has remained unresolved. For this reason, it is imperative to minimize the external variability and rigorously control experimental conditions, allowing the specific effects of factors—such as liquid chemistry—on triboelectric performance to be isolated and accurately assessed.

Historically, scientists have introduced the triboelectric series (Figure 1), which ranks materials based on their tendency to gain or lose electrons upon contact. However, many researchers argue that the series lacks quantitative evidence, shows poor reproducibility, and fails to adequately explain numerous TE phenomena (5, 9, 12). As such, several alternative mechanisms have been proposed in recent years.

Wang et al. (2019) proposed that electron transfer driven by electron cloud overlap during contact is a universal mechanism applicable to solids, liquids, and gases (5). In contrast, Yang et al. (2023) suggested that TE involved not only electron transfer, but also a mechanochemically driven radical anion transfer, which may account for the persistence of long-lived charges (6). For liquid-solid interfaces, other studies emphasized ion transfer, acid-base interactions, and electrical double-layer rearrangement as dominant contributors to charge transfer (13–15). A recent study by Yoo et al. (2023) presented a new liquid triboelectric series that classified liquids by their TE charging tendencies; however, further research is needed to confirm the reproducibility of these findings (16).

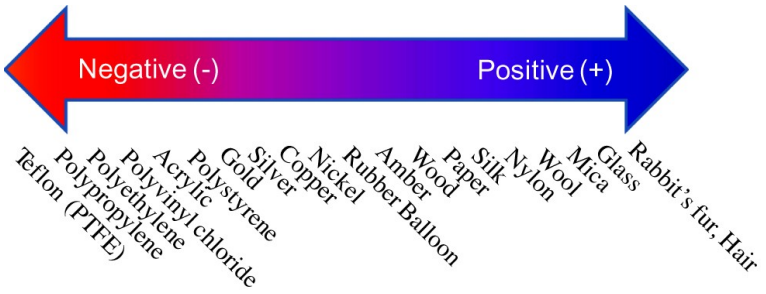

Figure 1. Depiction of the triboelectric series. Materials positioned on the positive side become positively charged upon contact with those on the negative side. Adopted from Lacks and Sankaran (2011).

Despite significant progress, the quantitative understanding of how solution chemistry, especially pH, affects charge generation in droplet-based triboelectric systems remains limited. This study investigated how changes in the pH of liquid droplets affect triboelectric charging on a polytetrafluoroethylene (PTFE) surface to understand the underlying charge-transfer mechanism. By analyzing changes in charge magnitude and polarity across acidic, neutral, and basic conditions, this work evaluates whether electrons, ions, or chemical absorbed species dominate charge transfer at the liquid-solid interface.

2. Materials and Methods

This experiment was designed to examine how the pH of a liquid affects triboelectric charge generation on a PTFE surface in a droplet-based TriboElectric NanoGenerator (TENG).

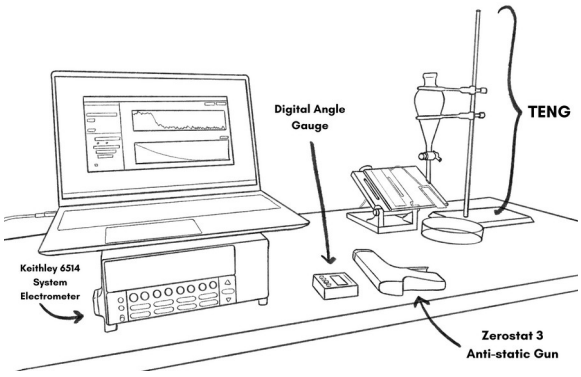

Figure 2. An overview of the experimental set-up and environment.

The set-up was constructed to isolate the effect of liquid properties on triboelectric performance under controlled conditions. Each session involved preparing solutions of defined concentrations, constructing a consistent solid-liquid TENG, and measuring charge output over time using an electrostatic voltmeter. An overview of the experimental set-up is shown in Figure 2.

2.1 Fabrication of TENG

The droplet-based TENG was assembled by mounting a glass funnel vertically above a PTFE surface, which was fixed at a thirty-degree angle on an acrylic base (Figure 3a). The funnel had a controllable valve to regulate the droplet release rate, maintained at a constant value throughout the whole experiment. The PTFE film acted as a charge-collecting surface, as PTFE is known for its strong tendency to gain negative charge in triboelectrification according to the TE series (Figure 1). A Petri dish was placed beneath the PTFE assembly to catch the droplets after they rolled down the surface.

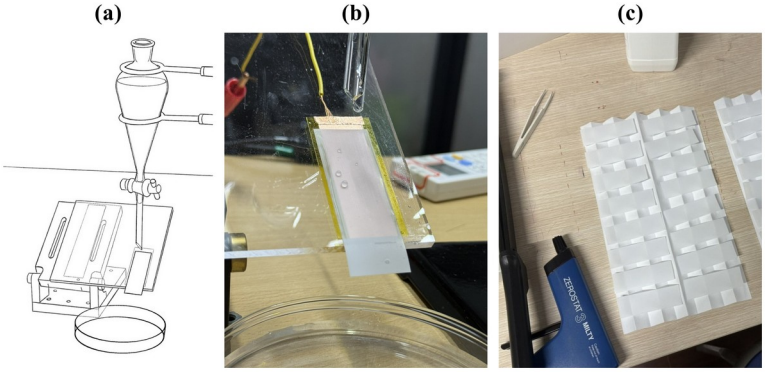

Figure 3. Experimental setup and surface preparation for droplet-based triboelectric measurements. (a) The droplet-based TENG configuration. (b) Close-up view of droplet-PTFE contact during sliding, illustrating the contact and separation process responsible for charge transfer. (c) PTFE surface treatment and neutralization procedure used to minimize residual charge.

2.2 Preparation of materials

A series of liquid solutions were prepared to evaluate the effect of solution composition and concentration on TE charge generation. To minimize the influence of the external variables, only one category of solution (acidic, basic, or organic) was prepared and tested per day. This approach reduced the risk of cross-contamination and ensured that all samples tested on the same day were subject to identical environment conditions. Distilled water was tested as a baseline control for each experimental day. A summary of all prepared solutions, including their composition and concentration rangers, is presented in Table 1.

Acetic acid and sodium acetate were used to generate acidic and basic solutions, respectively, over wide concentration ranges. Ethanol–water mixtures (1–10% v/v) were included to examine how reduced polarity and organic content influence droplet charging. Finally, mixed acetic acid–sodium acetate solutions were prepared to compare acidic and basic effects under controlled, partially neutralized conditions.

Polytetrafluoroethylene (PTFE) films were treated in a controlled manner to ensure consistent surface properties before experimentation. PTFE strips (3 cm x 7 cm) were rinsed thoroughly with distilled water to remove dust and surface contaminants. The films were then dipped in a hydrofluoroether

solution to displace any residual water that could generate charge on the film's surface. After this treatment, the PTFE strips were placed on top of a folded piece of paper to dry, which minimized the contact area between the film and other materials during drying (Figure 3c). A Zerostat 3 anti-static gun was used to neutralize any remaining surface charge on the PTFE films after the placement. The treated films were left to dry in this setup and stored in a covered container until being used in the droplet impact experiment.

Table 1. Summary of solution types, solutes, concentrations, and solvents used during the experiment.

Solution Type	**Solute(s)**	**Concentrations**	**Solvent**
Acidic solutions	Acetic acid (CH_3COOH)	1 mmol/L, 200 mmol/L, 500 mmol/L	Water
Basic solutions	Sodium acetate (CH_3COONa)	0.5 mmol/L, 1 mmol/L, 5 mmol/L, 10 mmol/L, 100 mmol/L, 1000 mmol/L	Water
Ethanol-water mixtures	Ethanol	1%, 5%, 10% (v/v)	Water
Mixed acid-base solutions	Acetic acid (CH_3COOH) + Sodium acetate (CH_3COONa)	CH_3COOH) fixed at 500 mmol/L; CH_3COONa at 0, 30, and 300 mmol/L	Water

In the present study, droplet volume, release height, and surface geometry were held constant within each experimental series, such that the Weber and Reynolds numbers remained approximately fixed for relative comparisons. However, hydrodynamic variations cannot be completely separated from chemical effects, particularly when solution composition alters surface tension or viscosity. Systematic variation of droplet impact parameters will be an important focus of future studies aimed at decoupling hydrodynamic and chemical contributions to triboelectric charging.

2.3 Measurement of triboelectric properties and data processing

Before each experimental session, the apparatus was thoroughly cleaned and dried to eliminate any residual moisture or contamination that could influence the charge measurements. The experiments were conducted in a controlled laboratory environment under stable, low humidity conditions (24°C ± 1°C).

The instantaneous charge generation between the liquid drop and the PTFE surface was measured using a Keithley 6514 System Electrometer. The electrometer was connected to a copper electrode underneath the PTFE film, while the reference terminal was grounded through the instrument chassis. The device had a sensitivity of ~ 10-14 C, with an integration time of 100 ms, and data was collected and transferred to a laptop through a General-Purpose Interface Bus (GPIB) connection for real-time visualization and subsequent analysis.

For each solution, four independent trials (n=4) were conducted to evaluate repeatability and reduce random error. Each trial consisted of one full charge-time measurement cycle, and after each trial, the used PTFE film was discarded then replaced to eliminate the effects of residual surface charge from previous runs. During film replacement, the PTFE strip was carefully handled using non-conductive tweezers to avoid contamination or unintentional contact electrification. Before and after each film was positioned onto the acrylic platform, the Zerostat 3 anti-static gun was shot again to neutralize any surface charges on both the PTFE and the surrounding area.

During testing, a droplet was released by removing the stopper from the top of the funnel, allowing the liquid to flow by gravity and roll down the PTFE film. This process initiated a charge transfer from the droplet to the PTFE film, and the droplet ended up in the Petri Dish to be discarded (Figure 3b). Each trial lasted ~ seven minutes to reach the maximum saturation point, with the electrostatic charge output being continuously recorded by the electrometer.

The pH for each solution was calculated using OLI Studio, which models equilibrium ion speciation and pH based on full-base dissociation. For each trial, the charge-time curve recorded by the electrometer was imported into OriginPro, where an exponential decay function, $Q(t) = A\,e^{-kt} + y_0$ was fitted, where *Q(t)* represents the measured charge as a function of time, *A* is a fitting constant, and y_0 is the asymptotic steady-state value. The fitting was applied empirically to facilitate consistent extraction of the steady-state charge plateau, defined here as $Q_{max} = y_0$. The exponential functional form was not intended to represent a specific physical relaxation mechanism, and no physical meaning was attributed to the decay constant *k*. Instead, the fitting curve served as a practical method for estimating Q_{max}.

3. Results

All charge–time curves in this section show the measured charge output ΔQ (in coulombs) as a function of time. Because the droplet contacted only a small portion of the 3 cm × 7 cm PTFE film during each trial, ΔQ represents the total charge transfer during the droplet contact–separation event. Each solution was measured by four independent trials, and the reported quantity corresponds to the average charge across these four trials. All curves were plotted starting from zero charge to indicate an initially uncharged PTFE surface.

Due to the inherent sensitivity of liquid–solid triboelectrification to environmental factors and surface history, quantitative comparisons were restricted to datasets collected within the same experimental session. Distilled water controls measured on the same day served as internal references. While qualitative trends could be compared across solution classes and experimental days, absolute values of Q_{max} were not interpreted quantitatively across different sessions.

3.1 Basic Solutions: sodium acetate

As shown in Figure 4a, all sodium acetate solutions produced charge-time curves that remained exclusively negative throughout the entire measurement period. Each solution reached a well-defined plateau region, and as the

sodium acetate concentration increased (from 0.5 mmol/L to 1000 mmol/L), the plateau values became progressively less negative, approaching zero. No positive charge region was observed at any concentration in this series.

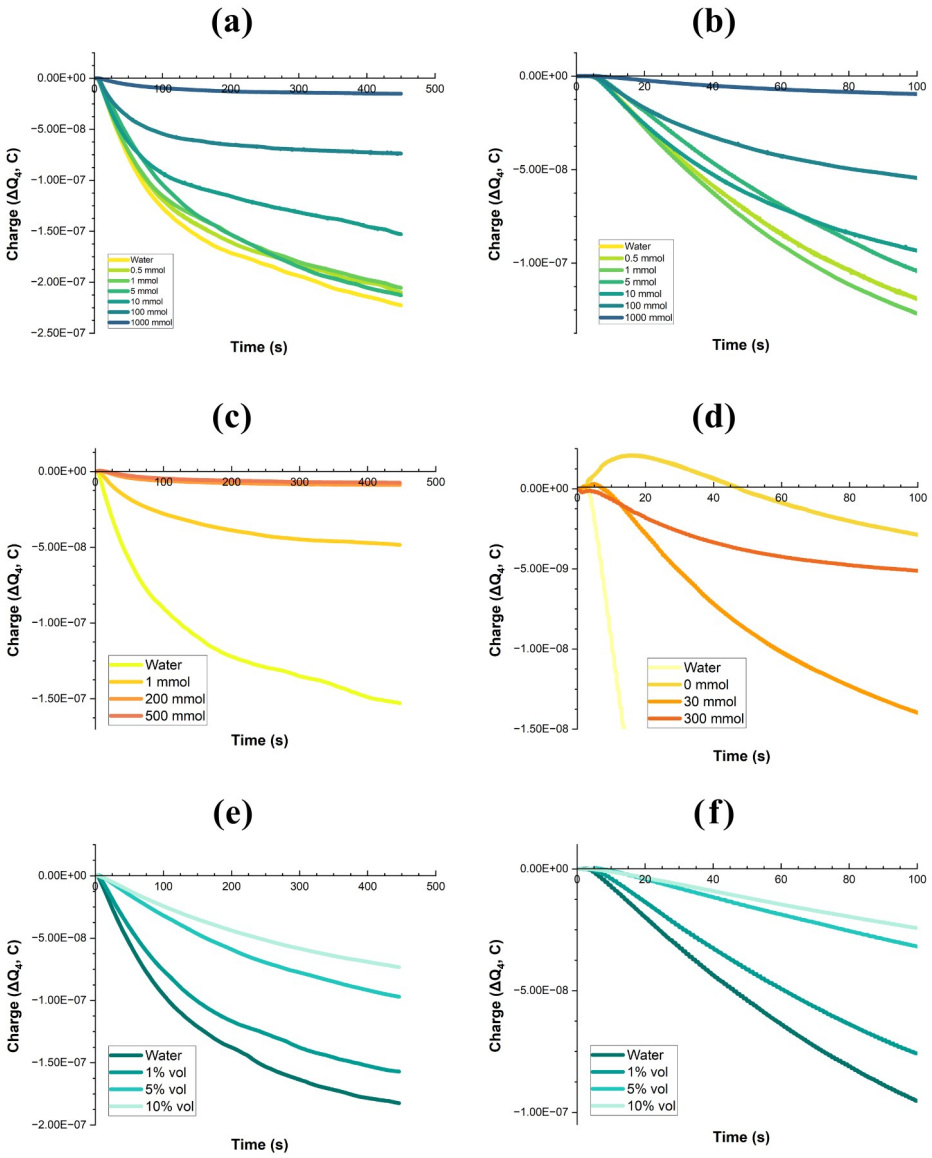

Figure 4. Charge–time response of a droplet-based PTFE triboelectric nanogenerator for different solution chemistries and concentrations. All curves represent the mean of four trials (ΔQ_4) and are scaled to start at zero at initial droplet contact. (a) Sodium acetate solutions over 500 s; (b) the first 100 s. (c) Acetic acid solutions over 500 s. (d) Mixed acetic acid–sodium acetate buffers in the first 100 s, highlighting suppression of the early-time positive charge region. (e) Ethanol–water mixtures over 500 s; (f) the first 100 s. Representative charge–time curves are shown for clarity; variability across trials is summarized in Table 2 using mean ± SD.

3.2 Acidic solutions: acetic acid

The acetic acid solutions in Figure 4c also demonstrated the same trend of the ΔQ becoming increasingly negatively charged until a plateau was reached. Interestingly, the acetic acid data had a distinct early-time feature not presented under the basic conditions. Each acetic acid solution generated an initial charge peak immediately after droplet contact, followed by a decay into the negative region. The magnitude of this early-time positive peak and the duration of the positive region changed systematically with acidity. For example, the 500 mmol acetic acid solution remained positive for about 50 seconds before transitioning to a negative plateau.

3.3 Mixed acid-base solutions

The charge-time curves for mixed acetic acid-sodium acetate solutions (Figure 4d) present the intermediate behavior between the purely acidic and purely basic cases. As sodium acetate was added to the acidic solutions, the initial positive peak decreased in magnitude. To highlight the early-time behavior, only the first 100 seconds of each charge-time curve are shown in Figure 4d. At higher acetate concentrations, the positive region during the first few seconds of charging disappeared entirely, and the charge-time curve resembled that of the sodium acetate solutions, remaining negative for the entire measurement.

3.4 Ethanol solutions

As shown in Figure 4e, ethanol-water mixtures did not generate any positive charge region. Their charge-time curves were similar to that of pure water, but the magnitude of the negative charge decreased with increasing ethanol percentage. For all the ethanol solutions, the charge remained negative across the entire duration of the measurement.

4. Discussion

4.1 General behavior and mechanism

Under all tested conditions, droplet contact with the PTFE surface produced measurable charge accumulation that evolved toward a stable negative plateau. This behavior is consistent with triboelectric charge accumulation observed in droplet-based TENG systems, where repeated contact and separation events lead to progressive charge buildup until electrostatic equilibrium is reached. While multiple mechanisms can contribute to liquid–solid charging, including electrokinetic effects, the persistence of charge polarity, saturation behavior, and agreement with the established triboelectric tendency of PTFE indicate that the observed charging is most consistent with triboelectric processes under the present experimental conditions.

The attainment of electrostatic equilibrium can be explained by models of Electric Double Layer (EDL) formation at the interface between a droplet and a dielectric surface, such as PTFE (1). Upon the initial droplet contact, rapid electron transfer is initiated, followed by rearrangement of counterions within the droplet at the charged interface—resulting in EDL formation (5, 13). As the droplet traverses the surface, the screening effect and the increment charge buildup gradually stabilize, manifesting as the observed charge plateau. The screening effect is governed by the Debye screening length (λ_D), which is inversely proportional to the

square root of the charged ion concentrations (I), $\lambda_D \propto I^{-1/2}$.

This relationship leads to a more compact electric double layer, which enhances electrostatic screening at the interface and limits sustained charge separation during droplet motion (7). Experimentally, all recorded charge outputs displayed negative values, indicating a net negative potential developing on the PTFE surface. Although the precise identity of the transferred species remains inconclusive in the current literature (4–9), the observed negative polarity is consistent with the triboelectric series, where PTFE is classified as a strongly electron accepting material (Figure 1). A notable exception, however, was observed for acidic droplets: the measured charge initially migrated into the positive region, persisted positively for a brief interval, then crossed zero to become negative (Figure 4d).

4.2 Influence of ionic and molecular species

A clear trend emerged when comparing the absolute values of $|Q_{max}|$ across all tested solutions: as the concentration of ionic or molecular species increased, the magnitude of total charge (ΔQ_{max}) accumulated on the PTFE surface decreased in comparison to distilled water. This behavior was observed for acidic, basic, mixed buffer, and ethanol–water systems, indicating that solution composition plays a central role in modulating liquid–solid triboelectric charging. The values summarized in Table 2 are used to illustrate these concentration-dependent suppression trends rather than to infer quantitative interfacial electrostatic parameters.

For electrolyte solutions, including acetic acid, sodium acetate, and mixed buffer systems, this suppression is consistent with enhanced ionic screening at the solid–liquid interface. As ionic concentration increases, counterions in the liquid more effectively redistribute near the charged PTFE surface, leading to compression of the interfacial electric double layer and attenuation of the local electric field. This increased screening reduces the effective driving force for continued charge separation and limits the accumulation of surface charge at steady state. In this context, the observed decrease in ΔQ_{max} with increasing electrolyte concentration is consistent with well-established electrostatic screening behavior at charged dielectric–liquid interfaces (1, 8, 15, 17).

In contrast, ethanol–water mixtures contain few mobile ionic species and therefore do not exhibit classical Debye-type screening behavior (19-21). Instead, increasing ethanol content modifies the dielectric environment and interfacial liquid structure at the PTFE surface. The ethanol lowers the effective dielectric permittivity of the solution, disrupts the hydrogen-bonding network of water, and modifies wetting and interfacial ordering. These effects weaken the stabilization of interfacial charges and reduce the efficiency of electron transfer during droplet contact and motion, leading to reduced triboelectric charge accumulation without inducing polarity reversal.

Despite these mechanistic differences, both electrolyte solutions and ethanol–water mixtures produce a common macroscopic outcome: progressive suppression of steady-

state charge accumulation with increasing solute concentration. In electrolytes, suppression arises primarily from ionic screening and interfacial charge redistribution, whereas in ethanol–water mixtures it is driven by reduced dielectric support and disruption of structured interfacial water layers. Taken together, these results suggest that the primary role of dissolved species is to modify interfacial electrostatic and molecular conditions that constrain net charge accumulation, rather than to act as the dominant transferred charge carriers at steady- state.

Table 2. Calculated (normal) pH and maximum accumulated charge (ΔQ_{max}) for acidic, basic, ethanol–water, and mixed buffer solutions tested on PTFE. Values are mean ± SD (n=4).

Solution Type	**Concentration**	**Calculated pH**	Q_{max} **± SD (nC)**
Water	Reference – acidic series		−149.8 ± 13.1
Acidic	1 mmol/L	3.920	−55.7 ± 1.1
	200 mmol/L	2.744	−8.6 ± 0.2
	500 mmol/L	2.545	−6.8 ± 0.4
Water	Reference – basic series		−229.7 ± 7.2
Basic	0.5 mmol/L	7.750	−205.8 ± 17
	1 mmol/L	7.893	−206.5 ± 16
	5 mmol/L	8.221	−206.5 ± 8.3
	10 mmol/L	8.359	−144.8 ± 12
	100 mmol/L	8.790	−72.0 ± 3.1
	1000 mmol/L	9.192	−18.8 ± 2.2
Water	Reference – ethanol series		−188.0 ± 3.6
Ethanol-water	1% (v/v)	7.014	−169.4 ± 12.9
	5% (v/v)	7.016	−121.2 ± 18.1
	10% (v/v)	7.019	−120.3 ± 15.7
Water	Reference – buffer series		Data was not recorded, as measurements were restricted to early-time transient effects.
Mixed Buffer	CH_3COOH 500 + CH_3COONa 0 mmol/L	2.545	
	CH_3COOH 500 + CH_3COONa 30 mmol/L	3.491	
	CH_3COOH 500 + CH_3COONa 300 mmol/L	4.363	

4.3 Influence of pH on the TE charging of PTFE

Because triboelectric charging at solid–liquid interfaces is known to be influenced by interfacial ion distributions (1, 14, 15), the acidity or basicity of each droplet was considered when examining the steady-state charge values (ΔQ_{max}). The pH of each solution was calculated using OLI Studio, and Table 2 summarizes these calculated values alongside the corresponding experimental charge measurements. The reported pH values represent calculated equilibrium estimates and

should be regarded as nominal rather than precise thermodynamic pH, particularly at high solute concentrations where non-ideal activity effects become significant. Accordingly, these values are used to contextualize trends across acidic, near neutral, and basic regimes rather than to define sharp transition thresholds. In addition, experimental pH measurements were not performed; therefore, all pH values should be interpreted as approximate model estimates.

Within these approximate regimes, droplets classified as acidic exhibited a transient positive charging phase during the early stages of contact that was absent under neutral and basic conditions. This behavior was evident in the charge–time responses of the mixed acetic acid–sodium acetate solutions (Figure 4d). Whereas neutral and basic droplets began accumulating negative charge on the PTFE surface immediately upon impact, acidic droplets displayed a brief excursion into the positive region before crossing zero and evolving toward the characteristic negative plateau. As the concentration of sodium acetate increases in solutions containing 500 mmol/L acetic acid, both the duration and magnitude of this transient positive feature decrease, indicating progressive suppression of the effect.

The trends summarized in Table 2 are consistent with these observations. Solutions within moderately acidic nominal pH ranges show small, short-lived positive deviations at early times, while more strongly acidic solutions display a more pronounced transient response. This behavior is consistent with increased proton availability near the interface, where proton enrichment and modification of the interfacial water layer may temporarily compete with electron-driven triboelectric charging during initial droplet–surface contact (13–15). As contact–separation proceeds, electron transfer becomes dominant, and the PTFE surface returns to its characteristic negative polarity.

This interpretation is consistent with previous studies by Sosa et al. (2020), who reported transient positive charging of PTFE and similar polymers upon interaction with sufficiently acidic droplets, while droplets at higher pH yielded exclusively negative charging behavior (23). The acetic acid droplets studied here fall within a transitional regime where both proton-mediated and electron-driven processes shape the early charging behavior, while the steady-state value of ΔQ_{max} reflects the electron-accepting nature of PTFE at equilibrium (5, 24).

While the transient positive charging observed under acidic conditions is consistent with short-lived proton accumulation at the solid–liquid interface, additional falsification experiments—such as pre-charging the PTFE surface or pre-conditioning with alkaline droplets—would provide more direct mechanistic validation. These tests are beyond the scope of the present study but represent promising approaches for future work to further distinguish proton-driven interfacial effects from alternative electrokinetic contributions.

The transient polarity reversal observed for acidic droplets may also have practical implications beyond steady-state energy harvesting. Since the positive signal appears at early contact times and precedes the negative

steady-state plateau, it provides time-domain information that is not accessible from equilibrium charge magnitude alone. Such early-time polarity features could enable rapid discrimination between acidic and non-acidic droplets, improving chemical selectivity in droplet-based triboelectric sensing platforms. More broadly, the transient response reflects kinetic interfacial processes that may be useful for probing solid–liquid interfacial chemistry or for triggering self-powered sensing functions. These potential applications, as shown in Table 3, were not explored experimentally in the present study but highlight opportunities for leveraging transient interfacial charge dynamics in future work.

Table 3. Practical applications of the transient polarity reversal in acidic droplets

Point	Domain	Transient-based capability	Potential application
1	**Chemical/ionic sensing**	Early-time positive polarity provides a rapid indicator of acidic droplets before steady-state charging develops	Self-powered acidity or aerosol sensing without electrodes.
2	**Selectivity in triboelectric sensors**	Transient polarity offers a distinguishing feature beyond steady-state magnitude, improving discrimination between acidic and neutral/basic droplets	Enhanced chemical selectivity in chemical or environmental sensing platforms
3	**Interfacial diagnostics & materials screening**	Transient behavior reflects proton affinity and interfacial water structuring at solid-liquid interface	Probing interfacial chemistry, evaluating surface treatments, coatings, and hydrophobic interfaces
4	**Event-triggering/ logic functions**	Early time polarity reversal can provide a distinct temporal signal separate from steady-state output	Self-powered triggers signals, timing/logic components in TENG systems

In contrast, droplets from basic-series and the ethanol–water mixtures did not exhibit this polarity reversal in their charge–time profiles (Figures 4b and 4f). This behavior is consistent with the limited tendency of acetate ions to accumulate at the hydrophobic PTFE interface and with the absence of a proton-adsorption phase under neutral or basic conditions (13, 24). As a result, charging in these systems is dominated primarily by electron transfer and ion screening rather than by interfacial chemical interactions.

Overall, these results demonstrated that TE charging of PTFE is governed not only by electron transfer and ion screening, but also by the acid-base chemistry at the solid-liquid interface. Acidic droplets introduce an interfacial proton accumulation mechanism, resulting in a transient positive charge that distinguishes their behavior from that of alkaline and neutral droplets, where the electron-transfer remains the primary mechanism responsible for the final negative charge accumulation on the PTFE surface (9, 25, 26).

4.4 Implications for the liquid triboelectric series

This experiment also provides a valuable insight into the development of the liquid triboelectric

series, which attempts to rank liquids by their charging tendency when contacting a solid surface, as discussed by Yoo et al. (2023) (16). In contrast to the well-established solid triboelectric series (Figure 1), a standardized liquid triboelectric series has yet to be established in the field (10).

The experimental results reported here support and extend recent observations within this area. The strong suppression of ΔQ_{max} at high solute concentrations indicates that a liquid's triboelectric "position" is not fixed. In both acidic and basic series, increased ionic strength compressed the EDL and reduced charge output, matching the findings that concentrated electrolytes display weaker triboelectric behavior (16). Therefore, ionic screening must be considered (kept consant or standardized) when comparing liquids in such a series.

Neutral liquids, such as ethanol-water mixtures, add further complexity. Despite having nearly the same pH as distilled water and lacking ions, increased ethanol content also causes a decrease in the produced charge. This charge decline is consistent with observations which note that solvents with disrupted hydrogen bonding or partial hydrocarbon character generate weaker triboelectric effects (16). Although this phenomenon was not addressed by Yoo et al. (2023), the solid-liquid trials in the study demonstrated that acidic water-based droplets displayed both positive and negative charge due to competing proton accumulation on the interfacial water layer. Acidity may thus influence a liquid's triboelectric output, but more experiments are necessary to confirm this hypothesis.

Ion-specific effects, including counterion size, valency, hydration, and Hofmeister ordering, are also expected to influence both the magnitude and kinetics of liquid–solid triboelectric charging by modifying interfacial water structure and screening efficiency. Although only acetate-based solutions were examined here, chaotropic and kosmotropic ions may differently affect transient charging behavior by altering interfacial hydrogen-bond networks. Systematic exploration of such ion-specific effects will be an important direction for future studies.

4.5 Competing mechanisms and boundaries of interpretation

Liquid–solid charge transfer can arise from several possible mechanisms, including triboelectric electron transfer, electrokinetic streaming currents, ion adsorption, or combinations of these processes. Each mechanism predicts distinct behaviors. Under triboelectric-dominant conditions, the charge polarity is governed primarily by the electron affinity of the solid surface and remains stable despite variations in droplet flow conditions, except when strong interfacial proton effects temporarily perturb the interface (9, 23, 24). Charge magnitude is expected to decrease with increasing ionic strength due to enhanced interfacial electrostatic screening (1, 8, 15).

In contrast, electrokinetic mechanisms predict different outcomes. Classical electrokinetic theory—summarized broadly in standard references such as Hunter's *Foundations of Colloid Science* and Probstein's *Physicochemical Hydrodynamics*—indicates that streaming currents depend on fluid motion,

reversing sign when flow direction reverses and increasing approximately linearly with flow velocity or shear. These frameworks provide the general physical expectations used here, although no specific equations or quantitative predictions from these texts are invoked.

Applying these contrasting predictions to the present system helps to clarify the mechanistic interpretation. For example, in an electrokinetic scenario, flow reversal would be expected to reverse the measured polarity, whereas in a triboelectric scenario the polarity should remain negative for PTFE regardless of flow direction (1, 8, 24). Although flow-reversal experiments were not performed, the persistence of negative polarity across all non-acidic solutions—despite substantial variations in chemistry—aligns more strongly with triboelectric behavior than with flow-dependent streaming currents.

Similarly, electrokinetic currents typically scale with flow velocity, whereas triboelectric charge accumulation commonly exhibits saturation behavior once contact–separation dynamics exceed the threshold for electron transfer. In this study droplet release height and flow rate were held constant, precluding direct assessment of velocity effects. Nonetheless, the strong dependence of charge magnitude on solution chemistry (ionic strength, acidity, ethanol fraction), rather than on geometric or hydrodynamic factors, supports triboelectric electron transfer coupled with interfacial screening rather than a velocity-controlled streaming-current mechanism (1, 13, 15).

Surface pre-charging provides another potential discriminating test. If early-time positivity in acidic droplets arises from proton enrichment, pre-charging the PTFE surface strongly negative would be expected to suppress or eliminate the transient positive excursion. However, steady-state polarity should remain negative because PTFE's high electron affinity dominates the final accumulated charge (24, 25). While such experiments were not performed here, the observed combination of transient positive charging followed by a robust negative plateau is consistent with this mixed proton/electron scenario.

Ion-specific effects also provide a means of distinguishing competing interpretations. Electrokinetic models generally predict modest variations among monovalent ions aside from hydration or adsorption differences, whereas triboelectric and interfacial-structural models anticipate stronger sensitivity to the Hofmeister series, particularly for chaotropic anions that disrupt interfacial water organization more strongly (13, 15). Although only acetate-based systems were examined in this work, the clear dependence of transient polarity on proton concentration—distinct from the monotonic screening behavior of sodium acetate solutions—indicates that early-time charging reflects interfacial proton processes rather than generic streaming currents. Future testing with chaotropic anions such as SCN^- could help clarify the interplay among interfacial water structure, proton mobility, and triboelectric charge transfer.

Taken together, the existing data are most consistent with triboelectric electron transfer governing the steady-state negative polarity, modulated by ionic screening and by

proton-mediated interfacial effects at low pH. Electrokinetic contributions cannot be completely ruled out without direct velocity or flow-reversal experiments; however, the absence of polarity reversal except under acidic conditions, the strong dependence on solution chemistry, and the agreement with PTFE's established electron-accepting behavior collectively support triboelectric dominance under the present experimental conditions.

4.6 Limitations

Although the trends observed in this study are internally consistent with the proposed interpretations of liquid-solid triboelectric charging, several limitations of this study should be acknowledged. First, due to the sensitivity of triboelectric charging to environmental conditions and surface history, quantitative comparisons are restricted to measurements conducted within the same experimental session using same-day water controls as internal references. Second, pH values are calculated equilibrium estimates and may deviate from true thermodynamic pH at high concentrations due to non-ideal activity effects. Third, parameters such as droplet volume, impact velocity, wetting dynamics, and surface roughness were held constant and were not systematically varied; thus, robustness and hydrodynamic sensitivity were not assessed. Finally, the present study focuses on a limited set of solution chemistries, and broader generalization will require controlled variation of ionic identity, flow direction, velocity, and surface pre-charging. These interpretive boundaries and their mechanistic consequences are discussed in Section 4.5.

5. Conclusion

Triboelectric nanogenerators (TENGs) are a promising pathway for harvesting small, otherwise wasted mechanical energies—such as falling droplets—and converting them into usable electrical power. Their ability to operate without another external power make them attractive candidates for self-powered sensors and environmental technologies. However, accurately predicting triboelectricity output remains challenging due to limited understanding of the underlying charge-transfer mechanisms.

This study investigates how solution chemistry and nominal pH influence charge generation on polytetrafluoroethylene (PTFE) surfaces under controlled droplet-based conditions. Across all tested solution types —including acidic, basic, mixed, and organic—the results consistently demonstrated that increasing solute concentration suppresses the magnitude of triboelectric charge. This trend indicates that dissolved species primarily act to modify and screen interfacial charge accumulation rather than serving as the dominant transferred charge carriers at steady-state. Under the present experimental conditions, the observed polarity persistence, saturation behavior, and agreement with the established triboelectric tendency of PTFE are most consistent with triboelectric charging being the primary contributor to the final accumulated charge, while acknowledging that secondary electrokinetic or hydrodynamic effects may also contribute.

A distinguishing feature of acidic droplets was the appearance of a transient positive charging phase during the initial moments of contact,

followed by a transition to the characteristic negative plateau. This behavior, observed over an approximate nominal pH range of 2.5–3.5, suggests that short-lived proton enrichment or modification of the interfacial water layer can temporarily compete with electron-driven triboelectric charging at early times. The absence of polarity reversal in basic and ethanol–water droplets further support the interpretation that proton-related interfacial effects play a unique role under acidic conditions, while electron transfer governs the steady-state charging response.

Future studies incorporating controlled factorial designs, ion-specific chemistry, hydrodynamic variation, and targeted falsification tests—such as surface pre-charging or chemical pre-conditioning—will be required to more rigorously decouple triboelectric, electrokinetic, and interfacial chemical contributions. Despite these limitations, the present results clarify how solution composition and nominal pH modulate both the magnitude and early-time behavior of liquid–solid charge transfer on PTFE surfaces. By emphasizing reproducible trends and clearly distinguishing steady-state charging from transient interfacial effects, this work contributes to a more coherent framework for understanding liquid-solid triboelectrification and informs the rational design of droplet-based TENG systems.

Acknowledgments

The author is grateful to Prof. Yao Yang and Dr. Jie Yang of the Department of Chemical and Biochemical Engineering at Zhejiang University, China, for providing laboratory facilities and resources that made this work possible.

6. References

1. Hu, Z., Gong, S., Chen, J., Guo, H. (2024). Energy harvesting of droplet-based triboelectric nanogenerators: From mechanisms toward performance optimizations. *DeCarbon*, 5, 100053. https://doi.org/10.1016/j.decarb.2024.100053

2. Lee, Y., Lee, M., Lee, J., Jang, H. W., Jang, J. S. (2025). Hydrovoltaic Power Generation Depend on Wettability at the Liquid-Solid Interface: Mechanisms, Materials, and Applications With Various Resource. *Exploration (Beijing, China)*, 5(2), 70007. https://doi.org/10.1002/EXP.70007

3. Sotthewes, K., Gardeniers, H. J. G. E., Desmet, G., Jimidar, I. S. M. (2022). Triboelectric Charging of Particles, an Ongoing Matter: From the Early Onset of Planet Formation to Assembling Crystals. *ACS Omega*, 7(46), 41828–41839. https://doi.org/10.1021/acsomega.2c05629

4. Fatti, G., Kim, H., Sohn, C., Park, M., Lim, Y.-W., Li, Z. et al. (2023). Uncertainty and Irreproducibility of Triboelectricity Based on Interface Mechanochemistry. *Phys. Rev. Lett.*, 131, 166201. https://doi.org/10.1103/PhysRevLett.131.166201

5. Wang, H., Huang, C.-C., Polcar, T. (2019). Controllable Tunneling Triboelectrification of Two-Dimensional Chemical Vapor Deposited MoS2. *Scientific Reports*, 9(1), 334. https://doi.org/10.1038/s41598-018-36830-1

6. Yang, P., Shi, Y., Tao, X., Liu, Z., Dong, X., Wang, Z. L. et al. (2023). Radical anion transfer during contact electrification and its compensation for charge loss in triboelectric nanogenerator. *Matter*, 6(4), 1295–1211. https://doi.org/10.1016/j.matt.2023.02.006

7. Arn, S., Illing, P., Harper, J., Burton, J. (2025). *The electrostatic charge on a falling water drop* (arXiv:2502.00159). *arXiv*. https://doi.org/10.48550/arXiv.2502.00159

8. Yuan, Z., Guo, L. (2024). Recent advances in solid-liquid triboelectric nanogenerator technologies, affecting factors, and applications. *Scientific Reports*, 14(1), 10456. https://doi.org/10.1038/s41598-024-60823-y

9. Lacks, D. J., Shinbrot, T. (2019). Long-standing and unresolved issues in triboelectric charging". *Nature Reviews Chemistry,* 3, 465–476. https://doi.org/10.1038/s41570-019-0115-1

10. Zou, H., Guo, L., Xue, H., Zhang, Y., Shen, X., Liu, X. et al. (2020). Quantifying and understanding the triboelectric series of inorganic non-metallic materials. *Nature communications*, 11(1), 2093. https://doi.org/10.1038/s41467-020-15926-1

11. Méndez Harper, J., McDonald, C. S., Rheingold, E. J., Wehn, L. C., Bumbaugh, R. E., Cope, E. J. et al. (2024). Moisture-controlled triboelectrification during coffee grinding. *Matter*, 7(1), 266–283. https://doi.org/10.1016/j.matt.2023.11.005

12. Mun, J.-H., Shin, E.-C., Seo, J., Kim, Y.-H. (2025). Triboelectric charge transfer theory driven by thermoelectric effect. *Phys. Rev. Res.*, 7, L032067. https://doi.org/10.1103/x3x7-s32f

13. Fu, J., Xu, G., Wu, H., Li, C., Zi, Y. (2022). Liquid-interfaces-based triboelectric nanogenerator: An emerging power generation method from liquid-energy nexus. *Advanced Energy and Sustainability Research*, 3(9), 2200051. https://doi.org/10.1002/aesr.202200051

14. Liu, Y., Liu, G., Bu, T., Zhang, C. (2021). Effects of interfacial acid–base on the performance of contact–separation mode triboelectric nanogenerator. *Materials Today Energy*, 20, 100686. https://doi.org/10.1016/j.mtener.2021.100686

15. Promsuwan, P., Hasan, M. A. M., Xu, S., Yang, Y. (2024). Droplet nanogenerators: Mechanisms, performance, and applications. *Materials Today*, 80, 497–528. https://doi.org/10.1016/j.mattod.2024.08.017

16. Yoo, D., Jang, S., Cho, S., Choi, D., Kim, D. S. (2023). A Liquid Triboelectric Series. *Advanced materials (Deerfield Beach, Fla.)*, 35(26), e2300699. https://doi.org/10.1002/adma.202300699

17. Feng, L., Wu, Y., Qu, J., Li, Z., Wang, J., Menon, C. (2025). Advancing liquid-solid triboelectric nanogenerators via micro/nano-structured interface engineering. *Composites Part B: Engineering*, 309, 113081. https://doi.org/10.1016/j.compositesb.2025.113081

18. Armiento, S., Filippeschi, C., Meder, F., Mazzolai, B. (2022). Liquid-solid contact electrification when water droplets hit living plant leaves. *Communications Materials*, 3(1). https://doi.org/10.1038/s43246-022-00302-x

19. Ranatunge, L., Rasekh, M., Ahmad, H., Balachandran, W. (2025). Impact of Ethanol on Electrostatic Behaviour of Fluorocarbon Pharmaceutical Propellants. *Pharmaceuticals*, 18(11), 1755. https://doi.org/10.3390/ph18111755

20. Wang, X., Ding, Z., Huang, C., Choi, K., Choi, D. (2025). Liquid-Solid Triboelectric Nanogenerators in Physical and Chemical Sensors-A Review. *Small*, 21(51), e06059. https://doi.org/10.1002/smll.202506059

21. Xia, K., Yu, M. (2025). Highly robust and efficient metal-free water cup solid–liquid triboelectric nanogenerator for water wave energy harvesting and ethanol detection. *Chemical Engineering Journal*, 503, 157938. https://doi.org/10.1016/j.cej.2024.157938

22. Li, S., Li, Y., Li, Q., Deng, Y., Fu, C., Xin, Y. et al. (2025). Screening nanogenerator based on the screening effect of water layer. *Nano Energy*, 137, 110827. https://doi.org/10.1016/j.nanoen.2025.110827

23. Sosa, M. D., Martínez Ricci, M. L., Missoni, L. L., Murgida, D. H., Cánneva, A., D'Accorso, N. B. et al. (2020). Liquid–polymer triboelectricity: chemical mechanisms in the contact electrification process. *Soft Matter*, 16, 7040–7051. https://doi.org/10.1039/D0SM00738B

24. Zhang, R., Olin, H. (2020). Material choices for triboelectric nanogenerators: A critical review. *EcoMat*, 2(4), e12062. https://doi.org/10.1002/eom2.12062

25. Horn, R. G., Smith, D. T., Grabbe, A. (1993). Contact electrification induced by monolayer modification of a surface and relation to acid–base interactions. *Nature*, 366(6454), 442–443. https://doi.org/10.1038/366442a0

26. Chen, Q., Shang, H., Cheng, B., Lu, C., Wang, Y., Zhang, Y. et al. (2024). Quantifying triboelectric series of polymers based on the measurement of triboelectrification with NaCl solution. *Chemical Engineering Journal*, 488, 150871. https://doi.org/10.1016/j.cej.2024.150871

27. Borjesson, A. (1995). A method for measurement of triboelectric charging. *Electrical Overstress/Electrostatic Discharge Symposium Proceedings*, 253–261. https://doi.org/10.1109/EOSESD.1995.478293

28. Lacks, D. J., Sankaran, R. M. (2011). Contact electrification of insulating materials. *Journal of Physics D: Applied Physics*, 44(45), 453001. https://iopscience.iop.org/article/10.1088/0022-3727/44/45/453001

29. Hunter, R. J. (2001) Foundations of Colloid Science, 2nd ed.; Oxford University Press: Oxford.

30. Probstein, R. F. (1994) Physicochemical Hydrodynamics, 2nd ed.; Wiley-Interscience: New York.